

The Physics of Deep-Inelastic Scattering at HERA

Cristinel Diaconu

*Centre de Physique des Particules de Marseille and
Deutsches Elektronen Synchrotron, Notkestrasse 85, 22607 Hamburg, Germany*

Abstract. In this paper an introduction to the physics of deep-inelastic scattering is given together with an account of some of the most recent results on the proton structure obtained in electron– and positron–proton collisions at the HERA collider.

Keywords: Deep inelastic scattering, proton structure, HERA collider , QCD.

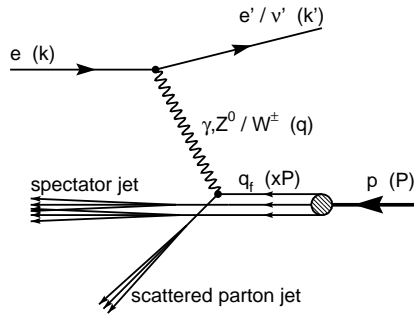
INTRODUCTION

The investigation of the matter structure using particle collisions started in early XX century with Geiger, Mardsen and Rutherford discovery of the atomic nucleus using α -particle scattering on a gold foil. The principle of the measurement is related to the spatial resolution obtained using high energy particles. The ‘resolving power’ can be expressed as $\delta \sim 200 \text{ MeV}/Q [10^{-15} \text{ m}]$ and is related to the uncertainty principle: the higher the transfer momentum (denoted by Q), the smaller the details that can be “flashed” and imprinted in the distribution of the scattered (point-like) particle. The search for further substructure levels continued with the scattering of leptons on light nuclei (H, D) in order to investigate the structure of protons and neutrons, the main components of the nuclear matter. The finite size of the proton was established in elastic scattering and its components, the quarks and the gluons, were discovered using electrons of higher and higher energies, which were ultimately able to break the nucleon in the so called deep inelastic scattering (DIS). In this paper, an introduction [1] to the physics of DIS is given using as examples recent measurements of the proton structure performed at HERA electron-proton collider¹.

THE OBSERVABLES OF LEPTON–HADRON SCATTERING

The lepton–hadron scattering is described in the framework shown in figure 1. The scattering can occur via the exchange of γ or Z bosons (neutral currents NC) or via W bosons (charged currents CC). In the later case, a neutrino is expected in the final state. The incoming electron (with a four-momentum k) scatters off the proton (P) to a final state electron with four–momentum k' via a virtual photon γ^* or a weak boson

¹ The paper is based on an introductory lecture presented at the “Carpathian Summer School of Physics on Exotic Nuclei and Nuclear/Particle Astrophysics”, August 20-31, 2007, Sinaia, Romania.



$$\begin{aligned}
 Q^2 &= -q^2 = -(k' - k)^2 \\
 y &= \frac{P \cdot q}{P \cdot k} \\
 x &= \frac{Q^2}{2P \cdot q} \quad (\text{Bjorken}) \\
 \nu &= \frac{P \cdot q}{M_p} \\
 W^2 &= (P')^2 = (P + q)^2 (= M_X^2) \\
 s &= (P + k)^2 (\text{fixed})
 \end{aligned}$$

FIGURE 1. Lepton-hadron scattering: an exchange of a boson in the t -channel.

with a virtuality Q^2 in the t -channel. The Bjorken variable x is associated with the fraction of the momentum of the proton carried by the struck parton. The total centre-of-mass energy is given by \sqrt{s} and the energy of the γ^*p system is given by W , which is equivalent to the total mass of the hadronic system in the final state M_X . In the case of elastic scattering $M_X = M_p$ and from M_X expression follows that $Q^2 = 2Pq$ and $x = 1$ (the whole proton interacts). Only two variables are independent, since the reaction is completely defined by the scattering angle and by the electron-parton centre-of-mass energy. The variable ν has a simple meaning in the proton rest frame, as the energy lost by the electron during the scattering $\nu = E_e - E'_e$, while y represents the fractional energy loss $y = \frac{E_e - E'_e}{E_e}$. Q^2 can be expressed as a function of the electron energy and scattered angle $Q^2 = 4E_e E'_e \sin^2 \frac{\theta}{2}$. From these relations, it is obvious that the DIS kinematics can be calculated from the measurement of the scattered electron only. The measurement of the hadrons in the final state, if available, can be exploited as an extra constraint or used in case of CC reactions, where the outgoing neutrino is not measured.

THE HERA PROJECT

The idea for a large electron-proton collider to mark a new step in the studies for proton structure, beyond the fixed target experiments, was promoted already in seventies [3]. The HERA collider project started in 1985 and produced the first electron-proton collisions in 1992. It is composed of two accelerators designed to store and collide counter rotating electrons (e^-) or positrons (e^+) with an energy of 27.5 GeV and protons with an energy of 920 GeV. The operations came to an end in June 2007 and the final analyses using the collected data are in progress at present.

HERA ring hosted two collider mode detectors H1 and ZEUS. They were built as hermetic (4π) multi-purpose detectors equipped with internal trackers able to measure charged particle momenta and calorimeters completing the measurement of the energy flow. Two other experiments used e^\pm or p beams for fixed target studies: HERMES, dedicated to the study of polarised $e^\pm p(N)$ collisions and (until 2003) HERA-B dedicated to the study of beauty production in hadronic collisions. Since 2003, the e^\pm beam were lon-

gitudinally polarised in collision mode with an average polarisation of $P_{e^\pm} = 30 - 40\%$. An integrated luminosity of 300^{-1} (200 pb^{-1}) has been collected in e^+p (e^-p) by each the two collider mode experiments, H1 and ZEUS.

DEEP-INELASTIC SCATTERING MEASUREMENTS AT HERA

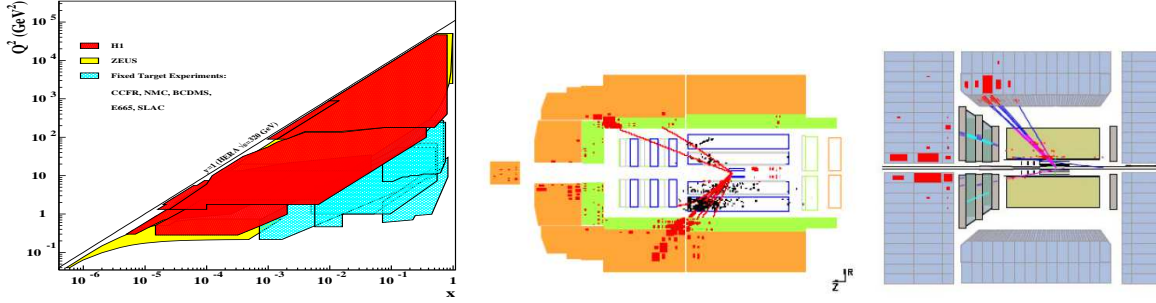


FIGURE 2. The kinematic plane accessible at HERA compared to former fixed target experiments (left) and event displays of a neutral current scattering event measured by H1 (center) and charged current scattering event measured by ZEUS (right).

The H1 and ZEUS experiments measured both neutral current (NC) and charged current (CC) processes. The kinematic (x, Q^2) plane accessible at HERA is shown in figure 2 (left) with a Q^2 domain up to 50000 GeV^2 and x down to 10^{-5} . The NC events contain a prominent electron and a jet of particles measured in the calorimeter, while in CC events only the jet is visible since the outgoing neutrino is not detected. Examples of such events are shown in figure 2.

Since a large domain in x and Q^2 is accessed, the NC cross section is sensitive to weak force effects. The proton structure, as revealed by the photon and Z^0 boson in DIS, can be incorporated into the so-called generalised structure functions. The cross section is parameterised as following:

$$\frac{d^2\sigma_{\text{NC}}^\pm}{dx dQ^2} = \frac{2\pi\alpha^2}{xQ^4} (Y_+ \tilde{F}_2 \mp Y_- x\tilde{F}_3 - y^2 \tilde{F}_L), \quad (1)$$

The generalised structure functions \tilde{F}_2 and $x\tilde{F}_3$ can be further decomposed as [4]

$$\tilde{F}_2 \equiv F_2 - v_e \frac{\kappa Q^2}{(Q^2 + M_Z^2)} F_2^{\gamma Z} + (v_e^2 + a_e^2) \left(\frac{\kappa Q^2}{Q^2 + M_Z^2} \right)^2 F_2^Z, \quad (2)$$

$$x\tilde{F}_3 \equiv -a_e \frac{\kappa Q^2}{(Q^2 + M_Z^2)} xF_3^{\gamma Z} + (2v_e a_e) \left(\frac{\kappa Q^2}{Q^2 + M_Z^2} \right)^2 xF_3^Z, \quad (3)$$

with $\kappa^{-1} = 4 \frac{M_W^2}{M_Z^2} (1 - \frac{M_W^2}{M_Z^2})$ in the on-mass-shell scheme [5]. The quantities v_e and a_e are the vector and axial-vector weak couplings of the electron or positron to the Z^0 [5]. The electromagnetic structure function F_2 originates from photon exchange only and dominates over the vast majority of the measured phase space. The functions F_2^Z and

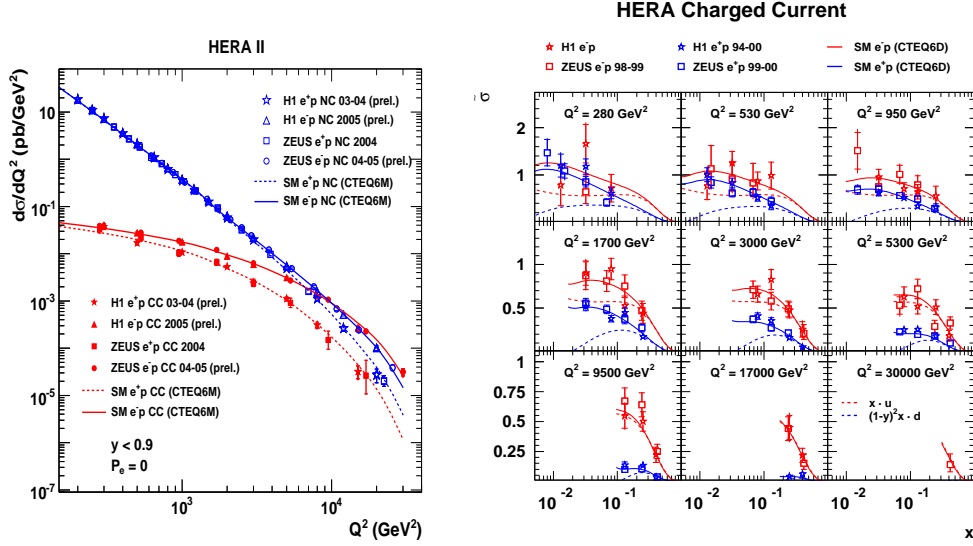


FIGURE 3. Left: the charged current and neutral current cross section as a function of Q^2 measured in $e^\pm p$ collisions at HERA. Right: the charged current reduced cross section $\tilde{\sigma}_{CC}$ as a function of x for various Q^2 values measured in electron– and positron–proton collisions.

xF_3^Z are the contributions to \tilde{F}_2 and $x\tilde{F}_3$ from Z^0 exchange and the functions $F_2^{\gamma Z}$ and $xF_3^{\gamma Z}$ are the contributions from γZ interference. These contributions are significant only at high Q^2 . The structure functions provide however direct information on the proton components. Within the so-called quark-parton model (QPM), the proton is composed of spin one half partons, called quarks $q = u, d$ with fractionary charges e_q . This model predicts the structure functions as combinations of quark densities $q(x)$. For instance $F_2 = \sum_q e_q q(x)$ and is independent of Q^2 (Bjorken scaling). This model is improved within the Quantum Chromodynamics (QCD) predicting quark interactions via gluons, the carriers of the strong force, and leading to F_2 dependence on Q^2 (scaling violation).

The charged current (CC) interactions, $e^\pm p \rightarrow \bar{\nu}_e X$, are mediated by the exchange of a W boson in the t channel. The cross section is parameterised as:

$$\frac{d^2\sigma^{CC}(e^\pm p)}{dx dQ^2} = \frac{G_F^2}{2\pi x} \left[\frac{M_W^2}{M_W^2 + Q^2} \right]^2 \tilde{\sigma}_{CC}^\pm(x, Q^2), \quad (4)$$

with $\tilde{\sigma}_{CC}^\pm(x, Q^2) = \frac{1}{2} [Y_+ W_2^\pm(x, Q^2) \mp Y_- x W_3^\pm(x, Q^2) - y^2 W_L^\pm(x, Q^2)]$. $\tilde{\sigma}$ is the reduced cross section, G_F is the Fermi constant, M_W , the mass of the W boson, and W_2 , xW_3 and W_L , CC structure functions. In the quark parton model, the structure functions W_2^\pm and xW_3^\pm may be interpreted as lepton charge dependent sums and differences of quark and anti-quark distributions: $W_2^+ = x(\bar{U} + D)$, $xW_3^+ = x(D - \bar{U})$, $W_2^- = x(U + \bar{D})$, $xW_3^- = x(U - \bar{D})$, whereas $W_L^\pm = 0$. The terms xU , xD , $x\bar{U}$ and $x\bar{D}$ are defined as the sum of up-type, of down-type and of their anti-quark-type distributions.

The differential NC and CC cross sections as a function of Q^2 are shown in figure 3 (left) for $e^\pm p$ collisions. At low Q^2 the NC cross section, driven by the electromagnetic interaction, is two orders of magnitude larger than the CC cross section

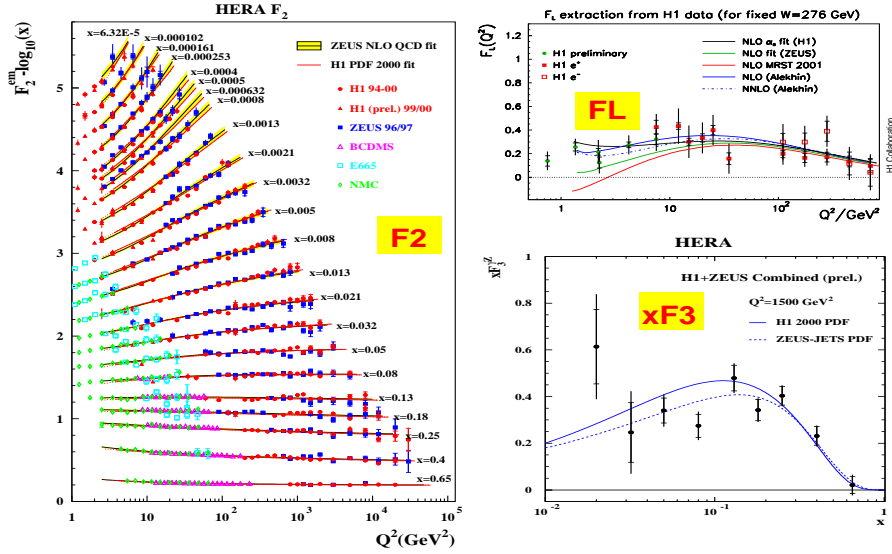


FIGURE 4. The determination of the structure functions F_2 , F_L and xF_3 from HERA measurements.

which correspond to a pure weak interaction. At large $Q^2 \sim M_{W,Z}^2$ the two cross sections are similar, which can be interpreted as a hint for electroweak unification. The largest Q^2 measurement corresponds to a resolution $\delta \simeq 10^{-18}$ m, i.e. 1/1000 the proton size. The agreement between the measurement and the prediction based on improved parton model constitutes a spectacular confirmation of QCD and suggests that no evidence for quark substructure is observed at present.

The double differential reduced cross section $\tilde{\sigma}_{CC}(x, Q^2)$ is shown in figure 3 (right). The CC processes are sensitive to individual quark flavours, especially visible at large Q^2 : the e^+p collisions probe the d quark distribution, while e^-p are more sensitive to the u distribution. This is a very useful feature of the CC processes compared to the NC, where the quark flavour separation is weaker.

STRUCTURE FUNCTIONS MEASUREMENTS: F_2 , F_L AND xF_3

The NC cross section is dominated over a large domain by the F_2 contributions, defined in equation 1. The measurement of the NC cross section at HERA can therefore be translated into an F_2 measurement, which is shown in figure 4 together with the previous measurements performed at fixed target experiments. One can observe the Bjorken scaling in the region at high x , but obvious scaling violation at lower x . This can be understood in terms of DGLAP equations [2] as a contribution driven by the gluon $\partial F_2(x, Q^2)/\partial \ln(Q^2) \approx (10\alpha_s(Q^2)/27\pi)xg(x, Q^2)$. while at high x the quark pdf's are the major contributors to the evolution in DGLAP equations.

From the F_2 measurements at fixed Q^2 one can observe a steep increase of F_2 towards low x , as shown in figure 5 (left). The region at low x is populated by quarks which have undergone a hard or multiple gluon radiation and carry a low fraction of the proton momentum at the time of the interaction. The observation of such large fluctuations to

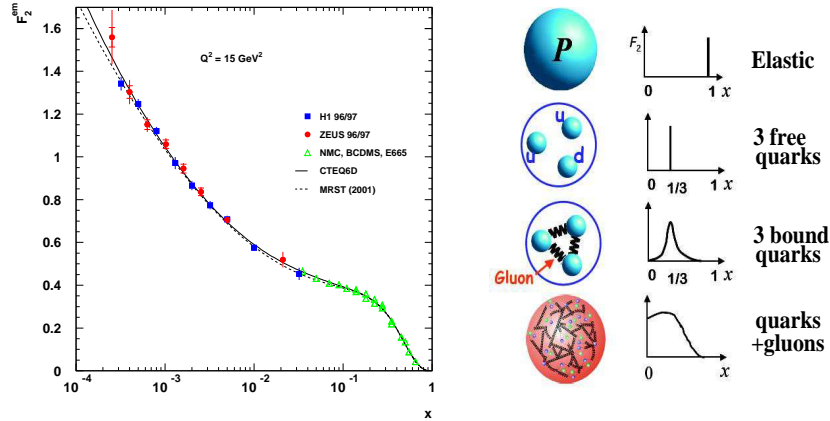


FIGURE 5. Left: The measurement of F_2 as a function of x for $Q^2 = 15 \text{ GeV}^2$. Right: a sketch of the correspondence between F_2 shape as a function of x and the quark-parton model.

very high parton density is driven by the uncertainty principle, which requires that the interaction time be very short and therefore at high Q^2 . In this regime, it is expected that the structure function grows at low x and shrinks at large x , confirmed by the experimental observation. The rise of the structure functions at low x is one of the most surprising observations at HERA. It is predicted in the double leading log limit of QCD [6]. It can be intuitively understood in terms of gluon driven parton production at low x , as depicted in figure 5 (right).

The longitudinal structure function F_L is usually a small correction, only visible at large y . The F_L measurement from the cross section has to proceed in such a way that F_2 contribution is separated. Indirect methods assume some parameterisation of F_2 to extract F_L . Using this method, an F_L determination can be performed and is shown in figure 4 at fixed W (the $\gamma^* p$ centre-of-mass energy). In the naive QPM the longitudinal structure function $F_L = F_2 - 2xF_1 \equiv 0$ and therefore F_L contains by definition the deviations from the Callan-Gross relation. It can be shown that F_L is directly related to the gluon density in the proton [7, 8] $xg(x) = 1.8[\frac{3\pi}{2\alpha_s}F_L(0.4x) - F_2(0.8x)] \simeq \frac{8.3}{\alpha_s}F_L$ meaning that at low x , to a good approximation F_L is a direct measure for the gluon distribution.

A direct measurement of F_L can be performed if the cross section $\sigma \sim F_2(x, Q^2) + f(y) F_L(x, Q^2)$ is measured at fixed x and Q^2 but variable y . This can only be performed if the centre-of-mass energy is varied, for instance by reducing the proton beam energy. Eliminating $F_2(x, Q^2)$, F_L can be directly measured with reduced uncertainties from the difference of cross sections: $F_L \sim C(y) * (\sigma(E_p^1) - \sigma(E_p^2))$. Measurements of DIS at HERA at lower proton energies of 460 GeV and 575 GeV has been performed at the end of the run in 2007 in order to perform the first direct measurement of F_L in the low x and high Q^2 regime.

The structure function $x\tilde{F}_3$ can be obtained from the cross section difference between electron and positron unpolarised data $x\tilde{F}_3 = \frac{Y_+}{2Y_-} [\tilde{\sigma}^-(x, Q^2) - \tilde{\sigma}^+(x, Q^2)]$. The dominant contribution to $x\tilde{F}_3$ arises from the γZ interference. In leading order QCD the inter-

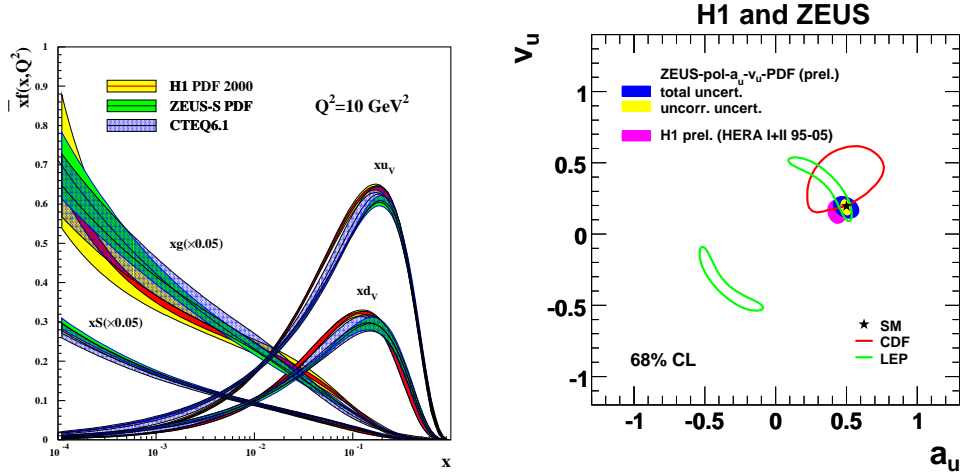


FIGURE 6. Left: The parton distribution functions extracted from HERA data. Right: Axial and vector couplings of the u -quark measured from the combined electroweak-QCD fit at HERA and compared with measurements from LEP (using light quarks production at Z pôle $e^+e^- \rightarrow q\bar{q}$) and Tevatron (from Drell-Yan electron pair production $q\bar{q} \rightarrow e^+e^-$).

ference structure function $xF_3^{\gamma Z}$ can be written as $xF_3^{\gamma Z} = 2x[e_u a_u(U - \bar{U}) + e_d a_d(D - \bar{D})]$, with $U = u + c$ and $D = d + s$ thus provides information about the light quark axial vector couplings (a_u, a_d) and the sign of the electric quark charges (e_u, e_d). The averaged $xF_3^{\gamma Z}$, determined by H1 and ZEUS for a Q^2 value of 1500 GeV^2 , is shown in figure 4.

PARTON DISTRIBUTION FUNCTIONS AND ELECTROWEAK EFFECTS

The NC and CC cross section measurements are used in a global fit in order to extract the parton distribution functions (pdf's) [9, 10]. The shapes for the quarks $q(x, Q_0^2)$ and gluon $g(x, Q_0^2)$ distributions are parametrised as a function of x at a given scale Q_0^2 and evolved using DGLAP equations [2] to each (x, Q^2) point where the cross section has been measured. The theoretical cross section can therefore be accurately calculated as a function of the pdf's parameters. A χ^2 is then built using the measurements and the predictions for all measurements points and minimised to extract the non-perturbative pdf's parameters. Since the number of parameters (typically 10) is much lower than the number of measurements (several hundred) the fit also constitutes a very powerful test of QCD. The structure functions from the fit are compared with data in figure 4. The parton distribution functions are extracted using the decomposition of the structure function described above. As an example, the pdf's obtained for $Q^2 = 10 \text{ GeV}^2$ are shown in figure 6. The valence distributions peak at $1/3$ as expected from simple counting with u_V twice as large as d_V . Gluon distribution is enhanced at low x . The knowledge of the proton structure deduced from inclusive CC/NC measurements can be used to calculate the cross section of exclusive processes leading to a specific final

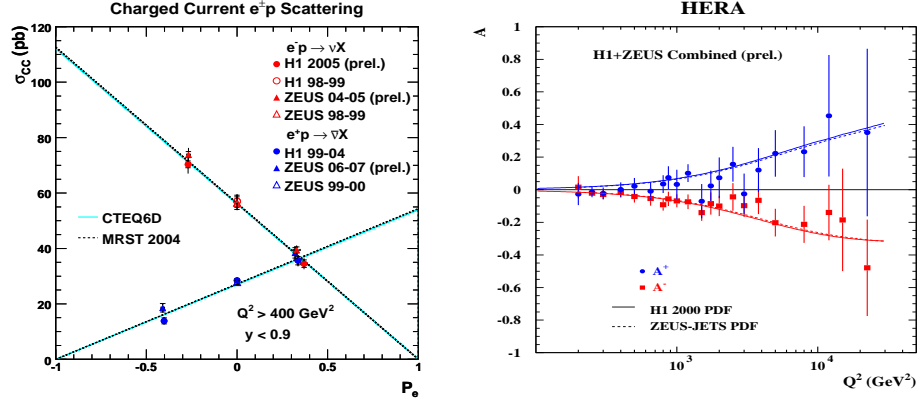


FIGURE 7. Left: The dependence of the charged current cross section on the electron or positron beam polarisation at HERA. Right: The polarisation asymmetry of the NC cross section at HERA.

state FS as a convolution of the parton level cross section with pdf's, for instance: $\sigma_{ep \rightarrow FS} = \sigma_{eq \rightarrow FS} \otimes q(x, Q^2)$. This factorisation can also be used to calculate the cross section of processes produced in proton–proton collisions using the pdf's measured in DIS.

Recently, a new approach has been adopted by the H1 and ZEUS collaborations[11], performing a combined QCD–electroweak fit. The strategy is to leave free in the fit the EW parameters together with the parameterisation of the parton distribution functions. Due to the t -channel electron-quark scattering via Z^0 bosons, the DIS cross sections at high Q^2 are sensitive to light quark axial (a_q) and vector (v_q) coupling to the Z^0 . This dependence includes linear terms with significant weight in the cross section which allow to determine not only the value but also the sign of the couplings. The measurements of the u -quark couplings obtained at HERA, LEP and Tevatron are shown in figure 6.

$e^\pm p$ COLLISION WITH A POLARISED LEPTON BEAM

The polarisation of the electron beam at HERA II allows a test of the parity non-conservation effects typical of the electroweak sector. The most prominent effect is predicted in the CC process, for which the cross section depends linearly on the e^\pm -beam polarisation: $\sigma^{e^\pm p}(P) = (1 \pm P)\sigma_{P=0}^{e^\pm p}$. The results[13] obtained for the first time in $e^\pm p$ collisions are shown in figure 7. The expected linear dependence is confirmed and provides supporting evidence for the V-A structure of charged currents in the Standard Model.

Due to parity violating couplings of the Z boson, the e^\pm beam polarisation effects can also be measured in NC processes at high Q^2 . The charge dependent longitudinal polarisation asymmetries of the neutral current cross sections, defined as

$$A^\pm = \frac{2}{P_R - P_L} \cdot \frac{\sigma^\pm(P_R) - \sigma^\pm(P_L)}{\sigma^\pm(P_R) + \sigma^\pm(P_L)} \simeq \mp k a_e \frac{F_2^{\gamma Z}}{F_2}, \quad (5)$$

measure to a very good approximation the structure function ratio. These asymmetries are proportional to combinations $a_e v_q$ and thus provide a direct measure of parity violation. In the Standard Model A^+ is expected to be positive and about equal to $-A^-$. At large x the asymmetries measure the d/u ratio of the valence quark distributions according to $A^\pm \simeq \pm k \frac{1+d_v/u_v}{4+d_v/u_v}$. The measurement from ZEUS and H1 [14], shown in figure 7, are in agreement with the theoretical predictions.

OUTLOOK

The study of deep-inelastic scattering is a fundamental branch of high energy physics. The structure of matter was last time resolved to new components, the quarks, in the first break-up of the proton at SLAC in 1968. Since then, the Standard Model of particle physics has become a well established theory with the last quark, the top, discovered in 1994. The knowledge of the structure of the baryonic matter, dominating the visible universe, has made huge progress in the last decades, thanks to an impressive effort to unravel the nucleon structure in fixed target experiments and at the HERA ep collider. The knowledge acquired at HERA is invaluable also for the physics of the Large Hadron Collider, foreseen to start pp collisions at 14 TeV in 2008. By enabling even more ambitious DIS experiments [15] beyond HERA, the matter structure investigations may gain a new momentum.

REFERENCES

1. More details about DIS physics can be found in the following monographies: R.K. Ellis, W.J. Sterling and B.R. Webber, "QCD and Collider Physics", Cambridge, ISBN 521 58189 3, (1996); R. Devenish and A. Cooper-Sarkar, "Deep Inelastic Scattering", Oxford University Press, ISBN13: 978-0-19-850671-3, (2005);
2. V.N. Gribov and L.N. Lipatov, Sov. J. Nucl. Phys. 15 (1972) 438, 675; L.N. Lipatov, Sov. J. Nucl. Phys. 20 (1975) 94; Yu. L. Dokshitzer, Sov. Phys. JETP 46 (1977) 641; G. Altarelli and G. Parisi, Nucl. Phys. B126 (1977) 298.
3. A. Febel, H. Gerke, M. Tigner, H. Wiedemann and B. H. Wiik, IEEE Trans. Nucl. Sci. **20** (1973) 782.
4. M. Klein and T. Riemann, Z. Phys. C **24** (1984) 151.
5. S. Eidelman *et al.* [Particle Data Group Collaboration], Phys. Lett. **B592** (2004) 1.
6. A. De Rújula *et al.*, Phys. Rev. D **10** (1974) 1649; R. D. Ball and S. Forte, Phys. Lett. B **336** (1994) 77 [arXiv:hep-ph/9406385]; R. D. Ball and S. Forte, Phys. Lett. B **335** (1994) 77 [arXiv:hep-ph/9405320].
7. G. Altarelli and G. Martinelli, Phys. Lett. B **76** (1978) 89.
8. A. M. Cooper-Sarkar *et al.*, Z. Phys. C **39** (1988) 281.
9. C. Adloff *et al.* [H1 Collaboration], Eur. Phys. J. C **30**, 1 (2003) [hep-ex/0304003].
10. S. Chekanov *et al.* [ZEUS Collaboration], Phys. Rev. D **67**, 012007 (2003) [hep-ex/0208023].
11. H1 and ZEUS Collaboration, contribution to EPS Conference, Manchester, UK, July 2007 [H1prelim-07-041, ZEUS-prel-06-003].
12. D. Acosta *et al.* [CDF Collaboration], Phys. Rev. D **71**, 052002 (2005) [hep-ex/0411059].
13. H1 and ZEUS Collaborations, contributions to EPS Conference, Manchester, UK, July 2007 [H1prelim-06-041, ZEUS-prel-06-003];
14. H1 and ZEUS Collaborations, contribution to EPS Conference, Manchester, UK, July 2007 [H1prelim-06-142, ZEUS-prel-06-022].
15. J. B. Dainton, M. Klein, P. Newman, E. Perez and F. Willeke, "Deep inelastic electron nucleon scattering at the LHC," JINST **1** (2006) P10001 [arXiv:hep-ex/0603016].